Exploiting Correlation Between Wideband and Differential CQIs for Adaptation and Feedback

Vineeth Kumar Neelesh B. Mehta, *Fellow, IEEE*

***Abstract*—Differential channel quality indicator (CQI) and wideband CQI are key components of the 4G and 5G standards. They enable a base station (BS) to acquire channel state information that is essential for rate adaptation and scheduling without overwhelming the uplink. We present a novel throughput-optimal rate adaptation rule, which exploits the correlation between the differential and wideband CQIs to improve throughput without any additional feedback, and a computationally efficient approach to evaluate it. We then propose a novel flexible-overhead differential CQI feedback scheme, in which the number of feedback bits can be subband-specific. The combination of the two approaches provides a new flexibility to the BS to control the feedback overhead and achieves a throughput comparable to conventional approaches with much less feedback.**

I. Introduction

Differential channel quality indicator (CQI) feedback is a critical component of both 4G long term evolution (LTE) and 5G standards, which refer to it as *higher layer-configured subband* (HLCS) feedback [1], [2]. It provides the channel state information that is essential for frequency-domain scheduling and rate adaptation by the base station (BS), while controlling the feedback sent on the resource-limited uplink channels.

In HLCS feedback, to reduce the feedback overhead, CQI is fed back at the frequency resolution of a subband, which comprises 24-96 adjacent subcarriers in 4G and 48-384 adjacent subcarriers in 5G. The feedback consists of a wideband CQI and differential CQI. The wideband CQI, which is encoded using 4 bits, is the index of the modulation and coding scheme (MCS) that can be reliably decoded if the entire system bandwidth is allocated to the user. For each subband, the differential CQI encodes using only 2 bits the difference between the index of the MCS that the user can reliably decode on that subband and the wideband CQI [3]. Despite these steps, the larger bandwidths used and the larger number of users that need to be serviced have led to feedback overhead becoming a significant bottleneck [4], [5].

A. Contributions

In this paper, we make the following contributions:

- We propose a novel *throughput-optimal MCS selection* (TOMS) rule for the BS. It specifies the throughput-optimal MCS to use in each subband given the wideband and differential CQIs. It exploits the correlation between these two CQIs in the sub-6 GHz bands of operation. The correlation occurs because the wideband CQI depends on each subband's signal-to-interference-plus-noise ratio (SINR). Furthermore, the large-scale shadowing and path-loss are the same for all subbands, even though the small-scale fading is not. To the best of our knowledge, this correlation has not been exploited in the literature. The TOMS rule chooses the MCS with the largest *feedback conditioned goodput*, which is the average number of bits that can be reliably decoded given the feedback. Since the exact expression for it is analytically intractable, we develop an accurate, computationally simpler approximation for it that applies to several multiple-input-multiple-output (MIMO) modes.
- We then propose a subband-level, flexible-overhead differential CQI feedback scheme, in which the number of bits for differential CQI can be different across the subbands. It differs from HLCS feedback in which a user always feeds back 2 bits per subband for differential CQI. In a multi-cell scenario, it achieves a throughput comparable to HLCS feedback with significantly less overhead. The judicious combination of wideband and differential CQIs, which are already employed in the standards, ensures that minimal modifications are needed to implement the proposed approach.

Comparison with Literature: Our approach differs from differential feedback for MIMO-orthogonal frequency division multiplexing (OFDM) systems in [6] and the references therein because these works do not model salient aspects of the 4G/5G standards such as differential and wideband CQIs, and rate adaptation. Differential techniques have been investigated in classical areas such as quantization [7, Ch. 3] and modulation [7, Ch. 5]. However, our model, analytical tools, and solution are all different. Our approach, which focuses on reducing the frequency-domain feedback overhead, is complementary to the approaches in [4] and [8], which exploit correlations in time and spatial domains. The TOMS rule is different from the sub-optimal conventional MCS selection rule (C-MSR), which is widely used in the related literature [3]–[5]. In C-MSR, the BS adds the wideband and differential CQIs to determine the index of the transmit MCS of each subband.

B. Organization and Notation

Section II presents the system model. Section III presents the TOMS rule and the feedback scheme. We present numer-

V. Kumar and N. B. Mehta are with the Dept. of Electrical Communication Eng. (ECE), Indian Institute of Science (IISc), Bangalore, India (Emails: vineethkumar01@gmail.com, nbmehta@iisc.ac.in).

This work was supported in part by the DST Swarnajayanti Fellowship Award under Grant DST/SJF/ETA-01/2014-15 and by the Indigenous 5G Test Bed Project funded by the Dept. of Telecommunications, India.

GLOBECOM 2020 - 2020 IEEE Global Communications Conference | 978-1-7281-8298-8/20/$31.00 ©2020 IEEE | DOI: 10.1109/GLOBECOM42002.2020.9348155

Authorized licensed use limited to: J.R.D. Tata Memorial Library Indian Institute of Science Bengaluru. Downloaded on May 12,2021 at 17:16:26 UTC from IEEE Xplore. Restrictions apply.

ical results in Section IV, and our conclusions in Section V.

Notation: We denote the probability of an event A by $\Pr(A)$ and the joint probability of events A and B by $\Pr(A, B)$. The conditional probability of A given B is denoted by $\Pr(A \mid B)$. We denote the probability density function (PDF) of a random variable (RV) X by $f_X(\cdot)$, its cumulative distribution function (CDF) by $F_X(\cdot)$, and the expectation with respect to X by $\mathbb{E}_X[\cdot]$. We denote the complex conjugate of a by a^* and its absolute value by $|a|$. The indicator function $1_{\{a\}}$ equals 1 if a is true and is 0 otherwise.

II. System Model

We consider the following system model that captures several key aspects of the OFDM-based downlink in LTE and 5G. A group of adjacent subcarriers constitutes a physical resource block (PRB). q adjacent PRBs constitute a subband. The number of subbands is B. A PRB comprises 12 subcarriers and a subband comprises 2 to 8 PRBs. A BS serves K users in the reference cell 0, which receives co-channel interference from C neighboring cells. The BS has N_t antennas and each user has N_r antennas.

Channel Model: The channel between a user and the BS undergoes frequency-selective, small-scale Rayleigh fading and large-scale shadowing. They are modeled as follows.

For user k, $H_{kn}^{(c)}(i,j)$ denotes the complex baseband downlink fading gain on subband n between transmit antenna j of BS c and receive antenna i of the user. It is a circularly-symmetric complex Gaussian RV with unit variance. $H_{kn}^{(c)}(i,j)$ are independent and identically distributed (i.i.d.) for different antennas i and j [9, Ch. 2]. Across the B subbands, $H_{k1}^{(c)}(i,j), \ldots, H_{kB}^{(c)}(i,j)$ are statistically identical but correlated. We use the exponential correlation model, in which the covariance of $H_{kn}^{(c)}(i,j)$ and $H_{kn'}^{(c)}(i,j)$ is $\rho^{2|n-n'|}$, where ρ is the correlation coefficient [10]. Later, we show how to apply our approach to any correlation model. For different k and c, $H_{kn}^{(c)}(i,j)$ are independent but non-identical RVs since the users can be at different distances from the BS.

The large-scale fading of the channel between user k and BS c is denoted by ω_{ck}. It is the same for all subbands [9, Ch. 1], [11]. In dB scale, ω_{ck} is a Gaussian RV with mean $\mu_{\omega_{ck}}(x_{ck}) = -\delta_{\text{dB}}(x_0) - 10\eta\log(x_{ck}/x_0)$ and standard deviation σ_{shad}, where x_{ck} is the distance between BS c and user k, $\delta_{\text{dB}}(x_0)$ is the path-loss at a reference distance x_0 from the BS, and η is the path-loss exponent [9, Ch. 1].

SINR: The following expression applies to several multi-antenna modes such as single-input-multiple-output (SIMO) with maximal ratio combining (MRC), multiple-input-single-output (MISO) with maximal ratio transmission, single-stream MIMO with MIMO beamforming, and multi-user MIMO with zero-forcing precoding. It enables a unified analysis. We explain it in detail for SIMO. We refer the reader to [3] for similar expressions for the other MIMO modes.

The SINR γ_{kn} on subband n of user k is [3]

$$\gamma_{kn} = \frac{P_T}{P_N}\frac{\omega_{0k}}{\varepsilon_{kn}}\phi_{kn}, \tag{1}$$

where P_T is the BS transmit power per subband and P_N is the additive white Gaussian noise (AWGN) power per subband. Here, $\phi_{kn} = \sum_{i=1}^{N_r} |H_{kn}^{(0)}(i,1)|^2$ is a gamma RV with parameters $d_k = N_r$ and $\lambda_k = 1$ that tracks the small-scale fading [12]. It has a PDF $f_{\phi_{kn}}(v) = v^{d_k - 1}e^{-\frac{v}{\lambda_k}}/(\Gamma(d_k)\lambda_k^{d_k})$, for $v \geq 0$, where $\Gamma(\cdot)$ is the gamma function [13, (8.310)]. The denominator term ε_{kn} equals

$$\varepsilon_{kn} = \frac{P_T}{P_N}\sum_{c=1}^{C}\omega_{ck}|I_{kn}(c)|^2 + 1, \tag{2}$$

where $I_{kn}(c) = \frac{\sum_{i=1}^{N_r}\left(H_{kn}^{(0)}(i,1)\right)^* H_{kn}^{(c)}(i,1)}{\sqrt{\sum_{i=1}^{N_r}|H_{kn}^{(0)}(i,1)|^2}}$ is a scaled version of the interference from BS l to user k on subband n. As shown in [14], it is a circularly-symmetric complex Gaussian RV with unit variance. Since ε_{kn} is a sum of lognormal RVs, which are modulated by exponential RVs, and 1, it is well approximated by a lognormal RV with parameters $\mu_{\varepsilon_{kn}}$ and $\sigma_{\varepsilon_{kn}}$ [3].

Therefore, γ_{kn} in (1) can be compactly written as

$$\gamma_{kn} = \Omega_k\phi_{kn}, \tag{3}$$

where Ω_k is a lognormal RV with parameters $\mu_{\Omega_k} = \mu_{\omega_{0k}}(x_{0k}) - \mu_{\varepsilon_{kn}} + \xi\log(P_T/P_N)$ and $\sigma_{\Omega_k} = \sqrt{\sigma_{\omega_{0k}}^2 + \sigma_{\varepsilon_{kn}}^2}$, and $\xi = 10/\log(10)$.

A. Discrete Rate Adaptation

The BS has an *MCS set* $\mathcal{M} = \{1, 2, \ldots, M\}$ of M MCSs. In it, MCS m has a rate r_m and a decoding threshold T_m. User k can decode it on subband n if $\gamma_{kn} \geq T_m$. Else, an outage occurs. Without loss of generality, let $0 = r_1 < r_2 < \cdots < r_M$ and $0 = T_1 < T_2 < \cdots < T_M < T_{M+1} = \infty$. For user k, the subband CQI Q_{kn} is the index of the highest-rate MCS that it can reliably decode on subband n, i.e.,

$$Q_{kn} = m, \quad \text{if } T_m \leq \gamma_{kn} < T_{m+1}. \tag{4}$$

For example, in LTE, there are $M = 2^4 = 16$ CQIs [1, Table 10.1]. LTE supports QPSK, 16QAM, and 64QAM modulation schemes and the rates after channel coding range from 0.15 to 5.55 bits/symbol. In 5G, there are three such MCS tables [2] and 256QAM is also supported.

The wideband CQI W_k is the index of the highest-rate MCS such that a codeword transmitted using it over the entire system bandwidth can be reliably decoded by user k [1, Ch. 10]. W_k is a single number that is reported for the entire bandwidth even though different subbands experience different, albeit correlated, fades. It can be systematically determined using the exponential effective signal-to-noise-ratio (SNR) mapping (EESM) [4], [15], [16]. EESM maps the vector $(\gamma_{k1}, \ldots, \gamma_{kB})$ of subband SNRs into a single effective SNR $\zeta_k^{(m)}$ for MCS m as follows:

$$\zeta_k^{(m)} = -\beta_m\log\left(\frac{1}{B}\sum_{n=1}^{B}\exp\left(-\frac{\gamma_{kn}}{\beta_m}\right)\right), \text{ for } m \geq 2, \tag{5}$$

Authorized licensed use limited to: J.R.D. Tata Memorial Library Indian Institute of Science Bengaluru. Downloaded on May 12,2021 at 17:16:26 UTC from IEEE Xplore. Restrictions apply.

TABLE I
IMPORTANT VARIABLES AND SYSTEM PARAMETERS

Parameters	Definitions
B	Number of subbands
N_t, N_r	Number of transmit and receive antennas
P_T, P_N	Transmit power of the BS and noise power per subband
M	Number of MCSs
r_m, T_m	Rate and decoding threshold for MCS m
γ_{kn}, $\zeta_k^{(m)}$	SNR of subband n, effective SNR for MCS m
Ω_k, ϕ_{kn}	Large-scale fading, small-scale fading on subband n
d_k, λ_k	Shape and scale parameters of gamma RV
W_k, D_{kn}	Wideband CQI and differential CQI for subband n

where β_m is an MCS-dependent scaling constant [4], [16]. $\zeta_k^{(m)}$ is interpreted as the equivalent SNR for MCS m that results in the same probability of error in an AWGN channel. W_k is then the highest-rate MCS for which $\zeta_k^{(m)} \geq T_m$. Thus,

$$W_k = m \text{ if } \zeta_k^{(m)} \geq T_m, \zeta_k^{(m+1)} < T_{m+1}, \ldots, \zeta_k^{(M)} < T_M, \quad \text{for } 2 \leq m \leq M. \quad (6)$$

Else, $W_k = 1$, which corresponds to zero rate (r_1).

The key notation is summarized in Table I.

III. FLEXIBLE DIFFERENTIAL FEEDBACK & TOMS RULE

We propose that user k encodes the difference $\Delta_{kn} = Q_{kn} - W_k$ for subband n using $b_{kn} \in \{0, 1, 2, 3, 4\}$ bits. The key point is that b_{kn} can be different for different subbands. The maximum is 4 bits because only 16 MCSs are defined for feedback in LTE and 5G [1, Ch. 10], [2]. Let the encoded value be D_{kn}, which we shall refer to as the differential CQI for subband n of user k. The values it takes depend upon b_{kn}.

The proposed encoding scheme for $b_{kn} \in \{1, 2, 3\}$ is specified in Table II.[1] (i) For $b_{kn} = 1$ bit, if $\Delta_{kn} \leq 0$, then $D_{kn} = 0$. Else, $D_{kn} = 1$. (ii) For $b_{kn} = 2$ bits, if $\Delta_{kn} \leq -1$, then $D_{kn} = -1$. If $\Delta_{kn} = 0$, then $D_{kn} = 0$. If $\Delta_{kn} = 1$, then $D_{kn} = 1$. Else, if $\Delta_{kn} \geq 2$, then $D_{kn} = 2$. The encoding for $b_{kn} = 2$ is kept the same as that in HLCS feedback, in which user k encodes Δ_{kn} using only $b_{kn} = 2$ bits for all n [1, Ch. 10]. The encoding for $b_{kn} = 3$ bits is specified in a similar manner. We refer to $\mathbf{D}_k = (D_{k1}, \ldots, D_{kB})$ as the vector of differential CQIs and $\mathbf{b}_k = (b_{k1}, b_{k2}, \ldots, b_{kB})$ as the *overhead bit pattern (OBP)*.

The user feeds back $\mathbf{D}_k$ and W_k to the BS. Hence, the total differential feedback overhead for user k is $O_k = \sum_{n=1}^{B} b_{kn}$ bits and the total feedback overhead including the 4-bit wideband CQI is $(O_k + 4)$ bits.

Implementation Aspects: The BS chooses the OBP $\mathbf{b}_k$ and communicates it to the user. This needs to be done only occasionally, i.e., every few tens of seconds, and higher-layer radio resource control signaling suffices for it. For example, the BS can do this when the loading in the cell changes.

[1]Two extreme cases need a special mention. First, for $b_{kn} = 4$ bits, Q_{kn} is reported as is without differential encoding since 4 bits are sufficient to indicate one among the 16 MCSs in the MCS table. Second, for $b_{kn} = 0$ bits, no feedback is sent for subband n.

A. TOMS Rule

We now determine the throughput-optimal downlink MCS $\tilde{S}_{kn}^*$ for subband n of user k. The rate achieved when MCS m is chosen is equal to $r_m 1_{\{\gamma_{kn} \geq T_m\}}$ because the user can decode it only if $\gamma_{kn} \geq T_m$. Therefore, the throughput given $\mathbf{D}_k$ and $W_k = w$ is

$$\mathbb{E}\left[r_m 1_{\{\gamma_{kn} \geq T_m\}} | \mathbf{D}_k, W_k = w\right] = r_m \Pr(\gamma_{kn} \geq T_m | \mathbf{D}_k, W_k = w). \quad (7)$$

We refer to $\Psi_{kn}^{(m)}(\mathbf{D}_k, w) = r_m \Pr(\gamma_{kn} \geq T_m | \mathbf{D}_k, W_k = w)$ as the *feedback-conditioned goodput* of MCS m on subband n. Hence, the throughput-optimal MCS $\tilde{S}_{kn}^*$ for subband n is

$$\tilde{S}_{kn}^* = \arg\max_{m \in \mathcal{M}} \left\{\Psi_{kn}^{(m)}(\mathbf{D}_k, w)\right\}. \quad (8)$$

Thus, in the TOMS rule, $\tilde{S}_{kn}^*$ is the index of the MCS that maximizes the feedback-conditioned goodput. Equation (8) also shows that C-MSR is sub-optimal since it determines the MCS $\tilde{S}_{kn}$ for subband n differently as $\tilde{S}_{kn} = W_k + D_{kn}$.

B. Computing Feedback-Conditioned Goodput

The main challenge lies in deriving an expression for $\Psi_{kn}^{(m)}(\mathbf{D}_k, w)$ that is tractable and has a low computational complexity. We set up the problem below. Given D_{kn} and $W_k = w$, it follows that $\gamma_{kn} \in [L_k(n), U_k(n))$, where $L_k(n)$ and $U_k(n)$ are the lower and upper thresholds of the SINR region in which γ_{kn} lies. This region can be easily inferred as follows: (i) From Table II, the BS identifies the condition for Δ_{kn} that corresponds to the given value of b_{kn} and the fed back D_{kn}. (ii) The condition in Δ_{kn} translates into a corresponding condition for Q_{kn} since $Q_{kn} = w + \Delta_{kn}$ (cf. Section III). (iii) From the condition for Q_{kn}, the BS then determines the range in which γ_{kn} lies using (4). For example, $b_{kn} = 2$ bits and $D_{kn} = -1$ implies that $\Delta_{kn} \leq -1$. This, in turn, implies that $Q_{kn} \leq w - 1$. From (4), we then get $\gamma_{kn} \in [0, T_w)$. When $b_{kn} = 0$ bits, $\gamma_{kn} \in [0, \infty)$.

Substituting the SINR regions for $\gamma_{k1}, \ldots, \gamma_{kB}$ in (7) yields

$$\Psi_{kn}^{(m)}(\mathbf{D}_k, w) = r_m \Pr\left(\gamma_{kn} \geq T_m | L_k(1) \leq \gamma_{k1} < U_k(1), \ldots, L_k(B) \leq \gamma_{kB} < U_k(B), W_k = w\right). \quad (9)$$

A closed-form expression for (9) is intractable. To avoid evaluating it numerically, which entails a large computational overhead, we present the following approximation. We shall verify its accuracy in Section IV.

Result *1:* Given the wideband and differential CQIs, $\Psi_{kn}^{(m)}(\mathbf{D}_k, w)$ is given by

$$\Psi_{kn}^{(m)}(\mathbf{D}_k, w) \approx \begin{cases} \frac{r_m E_m(w,n)}{G_m(w,n)}, & T_m < U_k(n), \\ 0, & T_m \geq U_k(n), \end{cases} \quad (10)$$

where $E_m(w, n)$ is the joint probability of the events $\gamma_{kn} \geq T_m$, $L_k(n) \leq \gamma_{kn} < U_k(n)$, and $W_k = w$, and $G_m(w, n)$ is

Authorized licensed use limited to: J.R.D. Tata Memorial Library Indian Institute of Science Bengaluru. Downloaded on May 12,2021 at 17:16:26 UTC from IEEE Xplore. Restrictions apply.

TABLE II
DETERMINATION OF DIFFERENTIAL CQI GIVEN THE NUMBER OF FEEDBACK OVERHEAD BITS

b_{kn} (bits)	D_{kn}	*Condition*	b_{kn} (bits)	D_{kn}	*Condition*
1	0	$\Delta_{kn} \leq 0$	3	-3	$\Delta_{kn} \leq -3$
	1	$\Delta_{kn} > 0$		-2	$\Delta_{kn} = -2$
2	-1	$\Delta_{kn} \leq -1$		-1	$\Delta_{kn} = -1$
	0	$\Delta_{kn} = 0$		0	$\Delta_{kn} = 0$
	1	$\Delta_{kn} = 1$		1	$\Delta_{kn} = 1$
	2	$\Delta_{kn} \geq 2$		2	$\Delta_{kn} \geq 2$
-	-	-		3	$\Delta_{kn} = 3$
				4	$\Delta_{kn} \geq 4$

the joint probability of the events $L_k(n) \leq \gamma_{kn} < U_k(n)$ and $W_k = w$. They are given by

$$\begin{aligned} E_m(w,n) = {} & \Pr\Big(\zeta_k^{(w)} \geq T_w, \gamma_{kn} \geq \max\left\{T_m, L_k(n)\right\}\Big) \\ & - \Pr\Big(\zeta_k^{(w)} \geq T_w, \gamma_{kn} \geq U_k(n)\Big) \\ & - \Pr\Big(\zeta_k^{(w+1)} \geq T_{w+1}, \gamma_{kn} \geq \max\left\{T_m, L_k(n)\right\}\Big) \\ & + \Pr\Big(\zeta_k^{(w+1)} \geq T_{w+1}, \gamma_{kn} \geq U_k(n)\Big), \end{aligned} \tag{11}$$

$$\begin{aligned} G_m(w,n) = {} & \Pr\Big(\zeta_k^{(w)} \geq T_w, \gamma_{kn} \geq L_k(n)\Big) \\ & - \Pr\Big(\zeta_k^{(w)} \geq T_w, \gamma_{kn} \geq U_k(n)\Big) \\ & - \Pr\Big(\zeta_k^{(w+1)} \geq T_{w+1}, \gamma_{kn} \geq L_k(n)\Big) \\ & + \Pr\Big(\zeta_k^{(w+1)} \geq T_{w+1}, \gamma_{kn} \geq U_k(n)\Big). \end{aligned} \tag{12}$$

Furthermore, for $w = M$, $\Pr\Big(\zeta_k^{(w+1)} \geq T_{w+1}, \gamma_{kn} \geq g\Big) = 0$, for all g.

Proof: The proof is relegated to Appendix A. ■

Every probability term in $E_m(w,n)$ and $G_m(w,n)$ is of the form $\Pr\Big(\zeta_k^{(l)} \geq T_l, \gamma_{kn} \geq g\Big)$. Note that the effective SINR $\zeta_k^{(l)} = -\beta_m \log\left(\frac{1}{B}\sum_{n=1}^{B} \exp\left(-\frac{\gamma_{kn}}{\beta_m}\right)\right)$ in the first term is correlated with γ_{kn} in the second term. Using the steps in [3, (16)–(32)], which we summarize below, it can be written in closed-form. We skip the derivations to conserve space.

1) $\Pr\Big(\zeta_k^{(l)} \geq T_l, \gamma_{kn} \geq g\Big)$ can be written as $\int_g^{\infty} \Pr\Big(\zeta_k^{(l)} \geq T_l | \gamma_{kn} = v\Big) \int_0^{\infty} f_{\Omega_k}(u)\, \frac{1}{u} f_{\phi_{kn}}\left(\frac{v}{u}\right) du dv$, where $f_{\Omega_k}(\cdot)$ is the PDF of the lognormal RV Ω_k and $f_{\phi_{kn}}(\cdot)$ is the PDF of the gamma RV ϕ_{kn}. Then, Gauss-Hermite quadrature [17, (25.4.46)] is used to simplify the inner integral.
2) $\Pr\Big(\zeta_k^{(l)} \geq T_l | \gamma_{kn} = v\Big)$ is evaluated in terms of the CDF of a Beta RV with parameters a_{li} and b_{li}, which are given below. The Beta RV arises because the term $\frac{1}{B}\sum_{n=1}^{B} \exp\left(-\frac{\gamma_{kn}}{\beta_m}\right)$, which is inside the exponential of the expression for the effective SNR $\zeta_k^{(l)}$ in (5), can be accurately approximated by it [15].
3) The Beta CDF is substituted in the outer integral in *Step 1*. Then, variable transformations, generalized Gauss-Laguerre quadrature [18], and simplifications yield the following final expression:

$$\begin{aligned} \Pr\Big(\zeta_k^{(l)} \geq T_l, \gamma_{kn} \geq g\Big) \approx {} & \frac{1}{\Gamma\left(d_k\right)\sqrt{\pi}} \sum_{i=1}^{\mathsf{GH}} z_i e^{\frac{-g}{\Lambda(\alpha_i)\lambda_k}} \\ & \times \sum_{p=0}^{d_k-1} \binom{d_k-1}{p} \left(\frac{g}{\Lambda(\alpha_i)\lambda_k}\right)^{d_k-1-p} \sum_{j=1}^{\mathsf{GL}} \tilde{z}_j^{(p)} \\ & \times \mathcal{B}\left(\frac{B}{B-1} e^{\frac{-T_l}{\beta_l}} - \frac{1}{B-1} e^{\frac{-\left(\lambda_k \tilde{\alpha}_j^{(p)}\Lambda(\alpha_i)+g\right)}{\beta_l}}; a_{li}, b_{li}\right), \end{aligned} \tag{13}$$

where $\Lambda(x) = e^{\left(\sqrt{2}\sigma_{\Omega_k} x + \mu_{\Omega_k}\right)/\xi}$, $\mathcal{B}\left(x; a, b\right) = \frac{\int_0^x z^{a-1}(1-z)^{b-1}\, dz}{\int_0^1 z^{a-1}(1-z)^{b-1}\, dz}$ is the regularized incomplete Beta function [13, (8.392)], $\tilde{z}_j^{(p)}$ and $\tilde{\alpha}_j^{(p)}$, for $1 \leq j \leq \mathsf{GL}$, are the weights and abscissas, respectively, of generalized Gauss-Laguerre quadrature [18], and z_i and α_i, for $1 \leq i \leq \mathsf{GH}$, are the weights and abscissas, respectively, of Gauss-Hermite quadrature [17, (25.4.46)].[2] The parameters a_{li} and b_{li} in (13), which define the Beta PDF [15], are given by

$$a_{li} = \mu_{li}\left[\mu_{li} - \left(\mu_{li}\right)^2 - V_{li}\right]/V_{li}, \tag{14}$$

$$b_{li} = \left(1 - \mu_{li}\right)\left[\mu_{li} - \left(\mu_{li}\right)^2 - V_{li}\right]/V_{li}. \tag{15}$$

Here, μ_{li} and V_{li} are the mean and variance, respectively, of the Beta RV, and are given by

$$\mu_{li} = \left(1 + \Lambda(\alpha_i)\lambda_k\beta_l^{-1}\right)^{-d_k}, \tag{16}$$

$$V_{li} = \left[\left(1 + 2\Lambda(\alpha_i)\lambda_k\beta_l^{-1}\right)^{-d_k} - \left(\mu_{li}\right)^2\right]/(B-1). \tag{17}$$

IV. PERFORMANCE EVALUATION AND BENCHMARKING

We evaluate the accuracy of Result 1 and compare different OBPs for different mean SNRs in Figs. 1 and 2. We then study the multi-cell scenario with co-channel interference, in which different users have different mean SNRs, in Fig. 3. We benchmark with the following combinations of feedback schemes and MCS selection rules used in the literature:

- *Full Channel State Information (CSI) [4]:* In it, for each subband, a user feeds back 4 bits to indicate the MCS to transmit on that subband. It yields the highest achievable throughput, but has the highest feedback overhead.
- *HLCS Feedback [1]–[4]:* In it, the differential encoding is done as per Table II with $b_{kn} = 2$ bits for all subbands. The BS uses C-MSR to determine the MCS for each subband.

The decoding thresholds T_m and the scaling constants β_m, for $1 \leq m \leq 16$, are as per [19, Table 1]. The decoding thresholds range from -9.5 dB to 19.8 dB, while the scaling constants range from 1 to 28.

[2]Generalized Gauss-Laguerre quadrature replaces $\int_0^{\infty} x^m e^{-x} f(x)\, dx$ with the finite summation $\sum_{j=1}^{\mathsf{GL}} \tilde{z}_j^{(m)} f\left(\tilde{\alpha}_j^{(m)}\right)$. Gauss-Hermite quadrature replaces $\int_0^{\infty} e^{-x^2} f(x)\, dx$ with $\sum_{i=1}^{\mathsf{GH}} z_i f(\alpha_i)$. To ensure numerical accuracy, $\mathsf{GL} = 8$ and $\mathsf{GH} = 10$ were found to be sufficient.

Authorized licensed use limited to: J.R.D. Tata Memorial Library Indian Institute of Science Bengaluru. Downloaded on May 12,2021 at 17:16:26 UTC from IEEE Xplore. Restrictions apply.

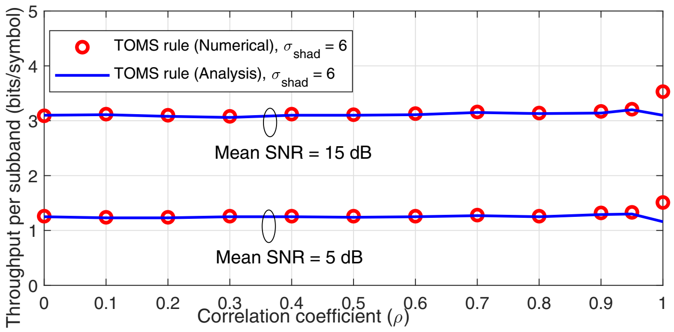

Fig. 1. Throughput per subband as a function of correlation coefficient ρ with OBP $(1,1,1,1,1,1,1,1,1,1)$ ($B=5$, $N_t=1$, and $N_r=2$).

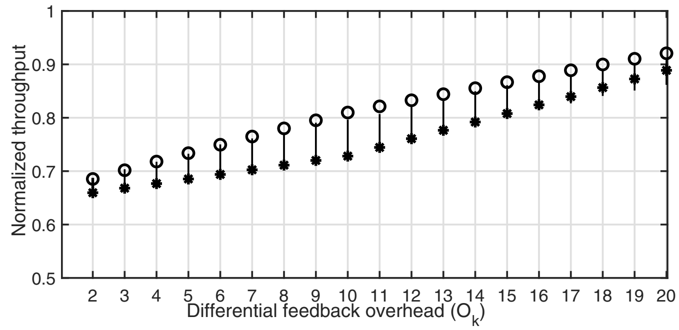

Fig. 2. Normalized throughput as a function of O_k (bits) for different OBPs ($B=10$, $\sigma_{\text{shad}}=6$, mean SNR of 15.3 dB, $\rho=0$, $N_r=2$, and $N_t=1$). The normalized throughput of the OBP that maximizes the throughput is shown using the marker '$\circ$'. For the best OBP, the normalized throughput with C-MSR is shown using the marker '$*$'. For each O_k, the vertical line shows the spread in the throughputs achieved by 20 randomly chosen OBPs.

Fig. 1 plots the throughput per subband that is achieved by the TOMS rule as a function of the correlation coefficient ρ between the subband channel gains. The OBP used is $(1,1,1,1,1,1,1,1,1,1)$. Also shown are the results when $\Psi_{kn}^{(m)}(\mathbf{D}_k,w)$ is computed numerically.[3] We see that the analysis, which captured the correlation between the wideband and subband CQIs and ignored ρ, is accurate for ρ as large as 0.95. The insensitivity of the throughput to ρ shows that the above correlation dominates the correlation across subbands due to small-scale fading.

Fig. 2 compares many OBPs and helps visualize the gains from using the TOMS rule. It plots the normalized throughput, which is the ratio of the throughput and the throughput with full CSI, as a function of the total differential feedback overhead O_k. For each O_k, the normalized throughput of the OBP that maximizes the throughput, which is found using a greedy search, is shown using the marker '$\circ$'. For this OBP, the normalized throughput with C-MSR is shown for comparison using the marker '$*$'. Also shown is the range of the normalized throughputs that are achieved by 20 randomly chosen OBPs with the TOMS rule and C-MSR. Since they are sub-optimal, they lie in a black vertical line below that of the optimal OBP. Given O_k, the length of the vertical line shows the throughput gain of the TOMS rule compared to C-MSR. For $O_k=20$ bits, the best OBP corresponds to that of HLCS feedback. However, this is not so for other values of O_k. For example, it is $(1,1,1,1,1,1,1,1,1,1)$ for $O_k=10$ bits and $(2,1,2,1,2,1,2,1,2,1)$ for $O_k=15$ bits.

As O_k increases, the normalized throughputs of all schemes increase since more CSI is fed back. The TOMS rule outperforms C-MSR for all O_k. The performance gap is most noticeable for $5 \leq O_k \leq 15$. The proposed approach yields 80% of the full CSI throughput and 95% of the throughput of HLCS feedback at a total overhead of 17 bits. This is only 42.5% of the full CSI feedback overhead of 40 bits. The high throughputs for $O_k < 20$ show the flexibility of the proposed scheme compared to HLCS feedback and its efficacy.

[3]In the numerical computation, we generate 10^6 channel realizations for each value of mean SNR. The conditional probability term in (10) is measured from these realizations.

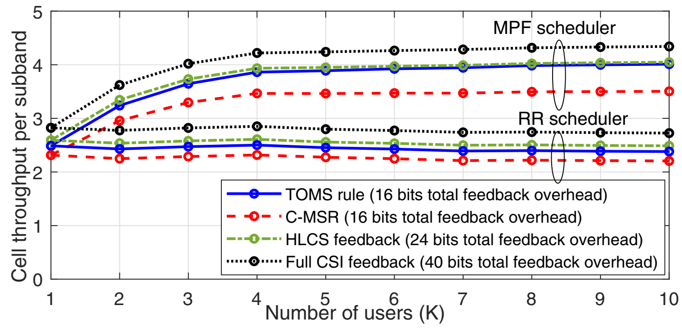

Fig. 3. Cell throughput per subband in bits/symbol as a function of K for MPF and RR schedulers ($B=10$, $\rho=0.86$, $N_t=1$, and $N_r=4$). The OBP $(1,2,1,1,1,1,1,1,2,1)$ is used for the TOMS rule and C-MSR.

A. Multi-Cell, Multi-User Scenario with Scheduling

We simulate a hexagonal cellular layout with $C=6$ interfering cells, cell radius of 300 m, and a frequency-reuse of one. The results are averaged over 2000 channel realizations and 200 drops of the users, whose locations are distributed uniformly in the reference cell except in a circular area of radius 30 m around the BS [11]. The path-loss parameters are $\eta=3.5$, $x_0=30$ m, and $\delta_{\text{dB}}(x_0)=10$ dB. P_T/P_N is set to get a cell-corner SNR of 3 dB.

Fig. 3 plots the cell throughput per subband of the TOMS rule and C-MSR as a function of K for the OBP $(1,2,1,1,1,1,1,1,2,1)$, for which the total feedback overhead, including wideband CQI, is 16 bits. We show results for the round-robin (RR) scheduler and the modified proportional fair (MPF) scheduler [4], [11], which selects the user that has the highest ratio of the feedback-conditioned goodput and its the mean value on that subband. The TOMS rule outperforms C-MSR for both schedulers. The throughput gain is larger for the MPF scheduler, especially for larger K, since the latter does not exploit multi-user diversity. With $K=10$, the MPF scheduler in conjunction with the TOMS rule achieves 92.3% of the cell throughput of full CSI feedback with just 40.0% of its total feedback overhead. The corresponding value for the

Authorized licensed use limited to: J.R.D. Tata Memorial Library Indian Institute of Science Bengaluru. Downloaded on May 12,2021 at 17:16:26 UTC from IEEE Xplore. Restrictions apply.

RR scheduler is 91.1%. For both schedulers, the throughput with the TOMS rule is very close to that of HLCS feedback with just 66.7% of its overhead.

V. Conclusions

We proposed a novel flexible-overhead feedback scheme that used wideband CQI and differential CQI. In it the number of overhead bits for differential feedback could be different for different subbands. We also derived an accurate low complexity approximation for the feedback-conditioned goodput of an MCS, which the TOMS rule maximized. The derivation accounted for small-scale fading, large-scale shadowing, co-channel interference, and multiple antenna modes, and exploited the correlation between the differential and wideband CQIs. The insensitivity of the proposed scheme to small-scale fading correlation implied that it can be used for the channel models specified in 3GPP. The proposed approach achieved a throughput comparable to the conventional HLCS feedback scheme with much less overhead for different schedulers.

Appendix

A. Sketch of Proof of Result 1

We use the intuition that given the wideband CQI $W_k = w$, limited additional information about $\tilde{S}^*_{kn}$ is conveyed by the feedback bits for other subbands. Using this and the Bayes' rule, (9) simplifies to

$$\Psi^{(m)}_{kn}(\mathbf{D}_k, w) \approx \frac{r_m \Pr(\gamma_{kn} \geq T_m, L_k(n) \leq \gamma_{kn} < U_k(n), W_k = w)}{\Pr(L_k(n) \leq \gamma_{kn} < U_k(n), W_k = w)}. \tag{18}$$

For $T_m > U_k(n)$, the events $L_k(n) \leq \gamma_{kn} < U_k(n)$ and $\gamma_{kn} \geq T_m$ are mutually exclusive. Hence, $\Psi^{(m)}_{kn}(\mathbf{D}_k, w) = 0$ for $T_m \geq U_k(n)$. For $T_m < U_k(n)$, (18) can be written as

$$\Psi^{(m)}_{kn}(\mathbf{D}_k, w) \approx r_m \frac{\begin{bmatrix} \Pr(W = w, \gamma_{kn} \geq \max\{T_m, L_k(n)\}) \\ - \Pr(W = w, \gamma_{kn} \geq U_k(n)) \end{bmatrix}}{\begin{bmatrix} \Pr(W = w, \gamma_{kn} \geq L_k(n)) \\ - \Pr(W = w, \gamma_{kn} \geq U_k(n)) \end{bmatrix}}. \tag{19}$$

Each term in (19) is of the form $\Pr(W_k = w, \gamma_{kn} \geq g)$. From (6), this common form can be written as

$$\Pr(W_k = w, \gamma_{kn} \geq g) = \Pr\left(\zeta^{(w)}_k \geq T_w, \zeta^{(w+1)}_k < T_{w+1}, \ldots, \zeta^{(M)}_k < T_M, \gamma_{kn} \geq g\right). \tag{20}$$

Computing it is still intractable as it requires an $(M - w + 2)$-dimensional joint PDF of the RVs $\zeta^{(w)}_k, \zeta^{(w+1)}_k, \ldots, \zeta^{(M)}_k$, and γ_{kn}. To simplify it, we observe it is highly unlikely that a user can decode higher-rate MCSs $(w + 2)$ and beyond if it cannot decode MCS $(w + 1)$. Therefore,

$$\Pr(W_k = w, \gamma_n \geq g) \approx \Pr\Big(\zeta^{(w)} \geq T_w, \zeta^{(w+1)} < T_{w+1}, \gamma_n \geq g\Big). \tag{21}$$

This implies that

$$\Pr(W_k = w, \gamma_{kn} \geq g) = \Pr\Big(\zeta^{(w)}_k \geq T_w, \gamma_{kn} \geq g\Big) - \Pr\Big(\zeta^{(w)}_k \geq T_w, \zeta^{(w+1)}_k \geq T_{w+1}, \gamma_{kn} \geq g\Big). \tag{22}$$

Using the same reasoning as above, we get

$$\Pr(W_k = w, \gamma_{kn} \geq g) \approx \Pr\Big(\zeta^{(w)}_k \geq T_w, \gamma_{kn} \geq g\Big) - \Pr\Big(\zeta^{(w+1)}_k \geq T_{w+1}, \gamma_{kn} \geq g\Big). \tag{23}$$

Applying the simplifications in (21)–(23) to each probability term in (19) yields (10).

References

[1] S. Sesia, I. Toufik, and M. Baker, *LTE – The UMTS Long Term Evolution, From Theory to Practice*, 2nd ed. John Wiley and Sons, 2009.

[2] "NR - Physical layer procedures for data," 3rd Generation Partnership Project (3GPP), TS 38.214, v16.0.0, 2019.

[3] V. Kumar and N. B. Mehta, "Modeling and analysis of differential CQI feedback in 4G/5G OFDM cellular systems," *IEEE Trans. Wireless Commun.*, vol. 18, no. 4, pp. 2361–2373, Apr. 2019.

[4] A. Chiumento, M. Bennis, C. Desset, L. Van der Perre, and S. Pollin, "Adaptive CSI and feedback estimation in LTE and beyond: A Gaussian process regression approach," *European J. Wireless Commun. Netw.*, vol. 2015, Jun. 2015.

[5] M. Cordina and C. J. Debono, "Robust predictive filtering schemes for sub-band CQI feedback compression in 3GPP LTE systems," *IET Commun.*, vol. 11, no. 11, pp. 1797–1807, Sep. 2017.

[6] Y. S. Jeon, H. M. Kim, Y. S. Cho, and G. H. Im, "Time-domain differential feedback for massive MISO-OFDM systems in correlated channels," *IEEE Trans. Commun.*, vol. 64, no. 2, pp. 630–642, Feb. 2016.

[7] J. G. Proakis, *Digital Communications*, 5th ed. McGraw-Hill, 2014.

[8] S. Homayouni, S. Schwarz, M. K. Mueller, and M. Rupp, "Reducing CQI feedback overhead by exploiting spatial correlation," in *Proc. IEEE VTC (Spring)*, Jun. 2018, pp. 1–5.

[9] G. L. Stüber, *Principles of Mobile Communications*, 2nd ed. Springer New York, 2011.

[10] V. A. Aalo and T. Piboongungon, "On the multivariate generalized gamma distribution with exponential correlation," in *Proc. IEEE Globecom*, Nov. 2005, pp. 1229–1233.

[11] J. Francis and N. B. Mehta, "Characterizing the impact of feedback delays on wideband rate adaptation," *IEEE Trans. Wireless Commun.*, vol. 14, no. 2, pp. 960–971, Feb. 2015.

[12] X. Yu, C. Li, J. Zhang, M. Haenggi, and K. Letaief, "A unified framework for the tractable analysis of multi-antenna wireless networks," *IEEE Trans. Commun.*, vol. 17, no. 12, pp. 7965–7980, Dec. 2018.

[13] L. S. Gradshteyn and L. M. Ryzhik, *Tables of Integrals, Series and Products*, 7th ed. Academic Press, 2007.

[14] A. Shah and A. M. Haimovich, "Performance analysis of maximal ratio combining and comparison with optimum combining for mobile radio communication with cochannel interference," *IEEE Trans. Veh. Technol.*, vol. 49, no. 5, pp. 1454–1463, Jul. 2000.

[15] J. Francis and N. B. Mehta, "EESM-based link adaptation in point-to-point and multi-cell OFDM systems: Modeling and analysis," *IEEE Trans. Wireless Commun.*, vol. 13, no. 1, pp. 407–417, Jan. 2014.

[16] J. C. Ikuno, M. Wrulich, and M. Rupp, "System level simulation of LTE networks," in *Proc. IEEE VTC (Spring)*, May 2010, pp. 1–5.

[17] M. Abramowitz and I. Stegun, *Handbook of Mathematical Functions with Formulas, Graphs, and Mathematical Tables*, 9th ed. Dover, 1972.

[18] P. Rabinowitz and G. Weiss, "Tables of abscissas and weights for numerical evaluation of integrals of the form $\int_0^\infty x^n e^{-x} f(x)\,dx$," *Mathematical Tables and Other Aids to Computation*, vol. 13, no. 68, pp. 285–294, 1959.

[19] J. Fan, Q. Yin, G. Y. Li, B. Peng, and X. Zhu, "MCS selection for throughput improvement in downlink LTE systems," in *Proc. ICCCN*, Jul. 2011, pp. 1–5.

Authorized licensed use limited to: J.R.D. Tata Memorial Library Indian Institute of Science Bengaluru. Downloaded on May 12,2021 at 17:16:26 UTC from IEEE Xplore. Restrictions apply.